Nuclear Engineering and Technology 53 (2021) 3314–3318

Contents lists available at ScienceDirect

Nuclear Engineering and Technology

journal homepage: www.elsevier.com/locate/net

Original Article

Electromagnetic interference caused by an electric-line current in a cable tray in nuclear power plants

Hoon-Keun Lee [a], Yong-Hwa Kim [b], Jaeyul Choo [c, *]

[a] Dept. of Safety Research, Korea Institute of Nuclear Safety, 62 Gwahak-ro, Yuseong-gu, Daejeon, 34142, Republic of Korea
[b] Railroad Management and Logistics and Computer Science, Korea National University of Transportation, 157 Cheoldobangmulgwan-ro, Uiwang-si, 16106, Republic of Korea
[c] Dept. of Electronics Engineering, Andong National University, 1375 Gyengdong-ro, Andong, 36729, Republic of Korea

ARTICLE INFO

Article history:
Received 19 December 2020
Received in revised form
9 April 2021
Accepted 11 April 2021
Available online 25 April 2021

Keywords:
Electromagnetic coupling
Mode-matching method
Open cable tray

ABSTRACT

This paper presents a mode-matching analysis of the electromagnetic coupling between open cable trays in an indoor structure when an electric-line current is generated as an electromagnetic source. We validated the mode-matching method by comparing the mode-matching results with those computed from a commercial electromagnetic simulator and then investigated the strength of the electric-field coupled in a victim cable tray while varying the distances between cable trays and architectural surfaces. The results of this study provide geometrical information on the placement of open cable trays to avoid electromagnetic interference problems.

1. Introduction

Cable trays play an important role in the protection of cables from external influences, such as undesired electromagnetic (EM) interference [1–4]. To apply the cable trays to a nuclear power plant, Regulatory Guide (Reg. Guide) 1.75, which is published by United States Nuclear Regulatory Commission, requires the physical independence of circuits/electrical equipment related to safety functions [5]. It endorses IEEE Std. 384, which describes specific criteria for the physical separation and electrical isolation of circuits/electrical equipment to meet this independence requirement [6]. To avoid the thermal effects of internal failures or faults in electrical equipment or cables, IEEE Std. 384 requires a minimum separation distance (D_v and D_h) between open cable trays placed in the limited hazard area of a nuclear power plant, as shown in Table 1. More specifically this standard recommends conducting EM analysis or testing to build an acceptable separation distance against unintended EM interference (EMI). In the indoor structure of a nuclear power plant, the scattering of the EM fields by the architectural surfaces (walls, ceiling, and ground) is one of crucial factors to determine EMI.

To evaluate this scattering of the EM fields, J Choo et, al [7]. have examined the EMI levels between the cable trays that are placed parallel (side-by-side) to each other at separation distances D_h of 25, 152, and 920 mm. In their work, the strength and distribution of the coupled electric field at the location in the victim cable tray were analyzed as function of the frequency and the shape of the cable tray. However, the EM coupling between the vertically placed cable trays has not been fully studied in the previous research. In the case that open cable trays are vertically stacked, the distance between cable trays (distance D_v in Table 1) is one of the most important factors to determine the EMI between open cable trays, which motivates us to perform this study.

Thus we, using a mode-matching method, have estimated the EM coupling intensity between open cable trays vertically installed in parallel to each other in a nuclear power plant. For the analysis, a vertical separation distance (D_v) of 305 mm between the cable trays was considered, and it was also assumed that the interfering EM field is generated by an inner electric-line current in the bottom cable tray. Differently from the previous study, our EM analysis focuses on predicting the EMI behavior while varying the separation distance from the indoor structure, such as the lateral walls, ceiling, and ground.

2. Mode-matching formulation

The mode-matching method is useful to analyze EM problems because it enables us to interpret the EM problem in terms of an individual mode, as well as efficiently derive the EM characteristics

* Corresponding author.
E-mail address: jychoo@anu.ac.kr (J. Choo).

https://doi.org/10.1016/j.net.2021.04.012

owing to the rapid convergence of the series solution. The mode-matching analysis is conducted in the following order: separation of the overall analyzed region, representation of EM fields using Helmholtz's equation in conjunction with separation of variables, and enforcement of boundary conditions on the tangential-field continuities between the separated regions.

Both open cable trays (cable trays 1 and 2) were simply modeled, as shown in Fig. 1, where the open cable trays (thickness t and the sizes $w \times h_1$ and $w \times h_2$) are placed in the separation distance c along the z-axis. We defined the bottom cable tray as the influencing cable tray having an EMI source and the upper cable tray as the victim cable tray affected by EMI, respectively. It was assumed that the cable trays are surrounded by lateral walls, ceiling, and ground made of a perfect electric conductor (PEC), as well as extended infinitely along the y-axis. In Fig. 1, the separation distances from the lateral walls, ceiling, and ground are defined as d_1, d_2, h_U, and h_G, respectively for surrounding design parameters. To express the sources of EM coupling, an electric-line current was set with strength J A/m^2 at ($x = \alpha_1$ and $z = \beta_1$). The overall region was divided into nine subregions (regions G, L_1, F_1, R_1, Q, L_2, F_2, R_2, and U) for formulating electric and magnetic fields. Then, the expression of the electric field in each subregion was derived by utilizing the Helmholtz equation, as follows [8].

Table 1
Minimum separation distances for limited hazard areas.

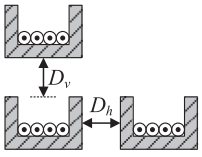	Interactions		
	Involving I&C cables only	Involving low-voltage power circuits with cable size ≤2/0 AWG	Involving low-voltage power circuits with cable size >2/0 AWG and all medium-voltage power circuit
Minimum D_h	25 mm	152 mm	920 mm
Minimum D_v	76 mm	305 mm	1530 mm

$$E_y^G(x,z) = i\omega \sum_{g=1}^{\infty} C_g \sin\gamma_g(x-x_1)\sin\xi_g(z-z_G) \tag{1}$$

$$E_y^{L_1}(x,z) = i\omega \sum_{l_1=1}^{\infty} \sin\gamma_{l_1}(x-x_1)(A_{l_1}\sin\xi_{l_1}z + B_{l_1}\cos\xi_{l_1}z) \tag{2}$$

$$E_y^{F_1}(x,z) = i\omega \sum_{f_1=1}^{\infty} C_{f_1} \sin\gamma_{f_1}(x-x_3)\sin\xi_{f_1}(z-z_{12}) \tag{3}$$

$$E_y^{R_1}(x,z) = i\omega \sum_{r_1=1}^{\infty} \sin\gamma_{r_1}(x-x_5)(A_{r_1}\sin\xi_{r_1}z + B_{r_1}\cos\xi_{r_1}z) \tag{4}$$

$$E_y^{Q}(x,z) = i\omega \sum_{q=1}^{\infty} \sin\gamma_q(x-x_1)(A_q\sin\xi_q z + B_q\cos\xi_q z) \tag{5}$$

$$E_y^{L_2}(x,z) = i\omega \sum_{l_2=1}^{\infty} \sin\gamma_{l_2}(x-x_1)(A_{l_2}\sin\xi_{l_2}z + B_{l_2}\cos\xi_{l_2}z) \tag{6}$$

$$E_y^{F_2}(x,z) = i\omega \sum_{f_2=1}^{\infty} \sin\gamma_{f_2}(x-x_3)\left(C_{f_2}\sin\xi_{f_2}(z-z_{22}) + S(2)\right) \tag{7}$$

$$E_y^{R_2}(x,z) = i\omega \sum_{r_2=1}^{\infty} \sin\gamma_{r_2}(x-x_5)(A_{r_2}\sin\xi_{r_2}z + B_{r_2}\cos\xi_{r_2}z) \tag{8}$$

$$E_y^{U}(x,z) = i\omega \sum_{u=1}^{\infty} A_u \sin\gamma_u(x-x_1)\sin\xi_u(z-z_U) \tag{9}$$

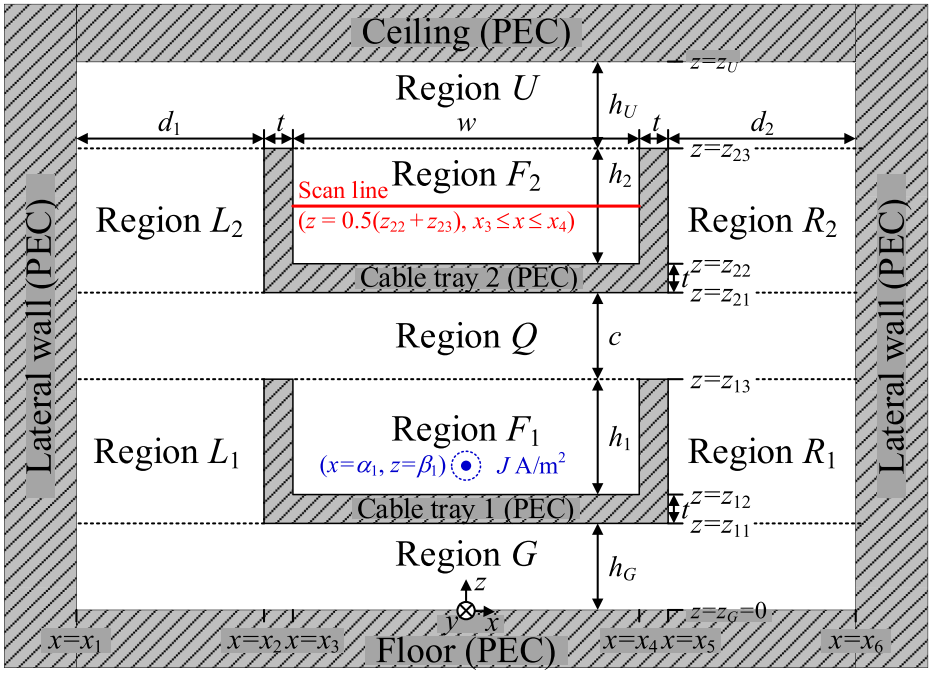

Fig. 1. Configuration of the cable trays.

where $S(n) = \begin{cases} X(n)\sin\xi_{f_n}(\beta - z_{n2})\sin\xi_{f_n}(z - z_{n3}) & , \ \beta < z \le z_{n3} \\ X(n)\sin\xi_{f_n}(\beta - z_{n3})\sin\xi_{f_n}(z - z_{n2}) & , \ z_{n2} \le z < \beta \end{cases}$, $X(n) = -2\mu_0 J \sin\gamma_{f_n}(\alpha - x_3)/(w\xi_{f_n}\sin\xi_{f_n}h_n)$, $\gamma_\chi = \chi/(x_6 - x_1)$, $\gamma_\sigma = \sigma/(x_2 - x_1)$, $\gamma_\psi = \psi/(x_4 - x_3)$, $\gamma_\tau = \tau/(x_6 - x_5)$, and $\xi_{\chi,\sigma,\psi,\tau} = \sqrt{k^2 - \gamma^2_{\chi,\sigma,\psi,\tau}}$ ($\chi = g, q,$ or u, $\sigma = l_1,$ or l_2, $\psi = f_1,$ or f_2, and $\tau = r_1,$ or r_2).

In addition, the magnetic field (H_x) in each region can be derived from the relation of $H_x = (i/\omega\mu)\cdot(dE_y/dz)$ [8].

The unknown modal coefficients A_α, B_β, and C_φ (α and $\beta = l_1, l_2, r_1,$ or r_2, and $\varphi = g, u, f_1,$ or f_2) in Eqs. (1)–(9) were determined by enforcing the boundary conditions on the continuities of the tangential electric and magnetic fields (E_y and H_x) at $z = z_{11}, z_{13}, z_{21},$ and z_{23}. At first, the continuities of the tangential electric and magnetic fields at $z = z_{11}$ are expressed as follows:

$$E_y^G(x,z)\Big|_{z=z_{11}} = \begin{cases} E_y^{L_1}(x,z)\Big|_{z=z_{11}} & , \ x_1 \le x < x_2 \\ 0 & , \ x_2 \le x < x_5 \\ E_y^{R_1}(x,z)\Big|_{z=z_{11}} & , \ x_5 \le x < x_6 \end{cases} \tag{10}$$

$$H_x^G\left(x,z\right)\Big|_{z=z_{11}} = H_x^{L_1}\left(x,z\right)\Big|_{z=z_{11}} \quad , \quad x_1 < x < x_2 \tag{11}$$

$$H_x^G\left(x,z\right)\Big|_{z=z_{11}} = H_x^{R_1}\left(x,z\right)\Big|_{z=z_{11}} \quad , \quad x_5 < x < x_6 \tag{12}$$

Secondly, the continuities of the tangential electric and magnetic fields at $z = z_{13}$ are expressed as follows:

$$E_y^Q\left(x,z\right)\Big|_{z=z_{13}} = \begin{cases} E_y^{L_1}\left(x,z\right)\Big|_{z=z_{13}} & , \ x_1 \le x < x_2 \\ 0 & , \ x_2 \le x < x_3 \\ E_y^{F_1}\left(x,z\right)\Big|_{z=z_{13}} & , \ x_3 \le x < x_4 \\ 0 & , \ x_4 \le x < x_5 \\ E_y^{R_1}\left(x,z\right)\Big|_{z=z_{13}} & , \ x_5 \le x < x_6 \end{cases} \tag{13}$$

$$H_x^Q\left(x,z\right)\Big|_{z=z_{13}} = H_x^{L_1}\left(x,z\right)\Big|_{z=z_{13}} \quad , \quad x_1 < x < x_2 \tag{14}$$

$$H_x^Q\left(x,z\right)\Big|_{z=z_{13}} = H_x^{F_1}\left(x,z\right)\Big|_{z=z_{13}} \quad , \quad x_3 < x < x_4 \tag{15}$$

$$H_x^Q\left(x,z\right)\Big|_{z=z_{13}} = H_x^{R_1}\left(x,z\right)\Big|_{z=z_{13}} \quad , \quad x_5 < x < x_6 \tag{16}$$

Thirdly, the continuities of the tangential electric and magnetic fields at $z = z_{21}$ are expressed as follows:

$$E_y^Q(x,z)\Big|_{z=z_{21}} = \begin{cases} E_y^{L_2}(x,z)\Big|_{z=z_{21}} & , \ x_1 \le x < x_2 \\ 0 & , \ x_2 \le x < x_5 \\ E_y^{R_2}(x,z)\Big|_{z=z_{21}} & , \ x_5 \le x < x_6 \end{cases} \tag{17}$$

$$H_x^Q\left(x,z\right)\Big|_{z=z_{21}} = H_x^{L_2}\left(x,z\right)\Big|_{z=z_{21}} \quad , \quad x_1 < x < x_2 \tag{18}$$

$$H_x^Q\left(x,z\right)\Big|_{z=z_{21}} = H_x^{R_2}\left(x,z\right)\Big|_{z=z_{21}} \quad , \quad x_5 < x < x_6 \tag{19}$$

Lastly, the continuities of the tangential electric and magnetic fields at $z = z_{23}$ are expressed as follows:

$$E_y^U\left(x,z\right)\Big|_{z=z_{13}} = \begin{cases} E_y^{L_2}\left(x,z\right)\Big|_{z=z_{23}} & , \ x_1 \le x < x_2 \\ 0 & , \ x_2 \le x < x_3 \\ E_y^{F_2}\left(x,z\right)\Big|_{z=z_{23}} & , \ x_3 \le x < x_4 \\ 0 & , \ x_4 \le x < x_5 \\ E_y^{R_2}\left(x,z\right)\Big|_{z=z_{23}} & , \ x_5 \le x < x_6 \end{cases} \tag{20}$$

$$H_x^U\left(x,z\right)\Big|_{z=z_{23}} = H_x^{L_2}\left(x,z\right)\Big|_{z=z_{23}} \quad , \quad x_1 < x < x_2 \tag{21}$$

$$H_x^U\left(x,z\right)\Big|_{z=z_{23}} = H_x^{F_1}\left(x,z\right)\Big|_{z=z_{23}} \quad , \quad x_3 < x < x_4 \tag{22}$$

$$H_x^U\left(x,z\right)\Big|_{z=z_{23}} = H_x^{R_2}\left(x,z\right)\Big|_{z=z_{23}} \quad , \quad x_1 < x < x_2 \tag{23}$$

After applying an orthogonal property to Eqs. (10)–(23), we can obtain 14 equations to constitute a set of simultaneous equations to determine the unknown modal coefficients. The modal coefficients can be calculated efficiently after truncating the infinite series in the simultaneous equations. The procedure to build a set of simultaneous equations from enforcing the boundary conditions is presented in the appendix of Choo's report [7].

3. Mode-matching results

For validation of the analysis, the electric-field distribution calculated by a mode-matching analysis was compared with that from a commercial EM simulator (COMSOL Multiphysics [9]) in a two-dimensional plane, as shown in Fig. 2. In Fig. 2, due to the structural symmetry with respect to the z–y plane, only halves of the electric-field distributions were represented with the mode-matching method (left) and the commercial EM simulator (right). The close similarity was shown between those electric-field distribution results (i.e., mode-matching method and COMSOL). For another validation of the analysis, the convergence of the series solution for the electric field was checked in each subregion. It was confirmed that the strength of an electric field quickly converges at the sample location as increasing the mode number in each subregion. These results imply a validation of the mode-matching formulation and computation.

The strength of an electric field along the scan line was investigated to examine the behavior of electric fields by varying the structure surrounding the cable trays. To evaluate quantitatively the EM coupling to the victim cable tray, the maximal allowable strength of the electric fields (E_{MA}) in a victim cable tray was defined as 4 V/m ($E_{MA} = 4$ V/m) [10].

Fig. 3 shows the variations in the electric-field strength on the scan line, which is shown in Fig. 1, at 500 MHz and 1 GHz while either the distance from the lateral walls (D_{LW}) or the distance from the ground and ceiling (D_{GU}) changes from 0.5 to 1 m. It is conceivable that the strength of the electric field coupled in the victim cable tray varies significantly depending on the distances D_{LW} and D_{GU}. Thus, these results reveal that the distance from a cable tray to the surrounding architectural structures (e.g., walls, ground, and ceiling) is one of the important factors to control the EM coupling in a victim cable tray.

For comparison of the results at 500 MHz and 1 GHz, Fig. 3 additionally shows that the strength of the coupled electric field at 500 MHz is lower than an E_{MA} of 4 V/m in all distances D_{LW} and D_{GU}, whereas that at 1 GHz is higher than the E_{MA} of 4 V/m in the several distances D_{LW} and D_{GU}. This result indicates that effective

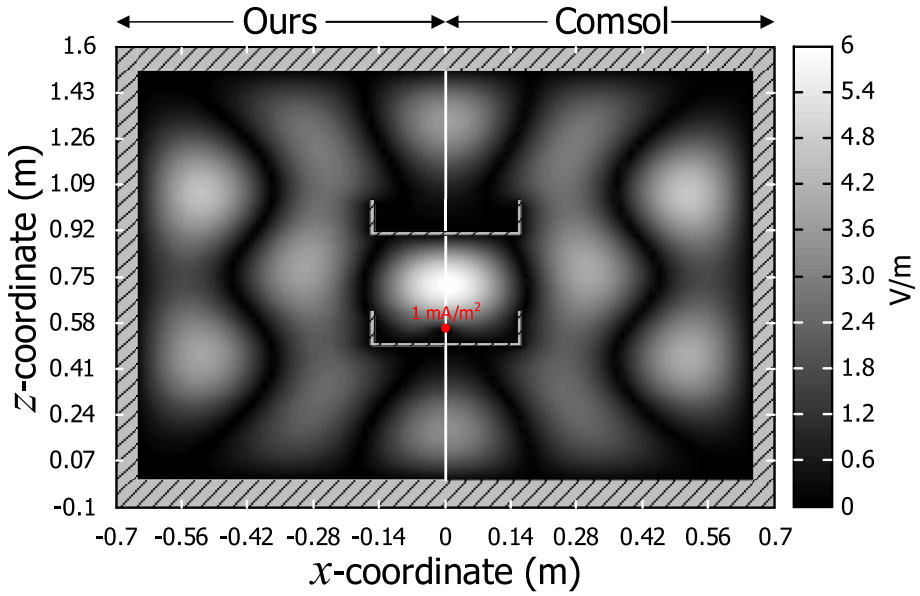

Fig. 2. Comparison of the electric-field distributions derived by a mode-matching method and a commercial EM simulator at 600 MHz ($J = 1$ mA/m^2, $\alpha_1 = (x_3 + x_4)/2$, $\beta = (z_{11} + z_{13})/2$, $d_1 = d_2 = h_G = h_U = 0.5$ m, $t = 0.005$ m, $w = 0.3048$ m (12 inch), $h_1 = h_2 = 0.1016$ m (4 inch), and $c = 0.305$ m).

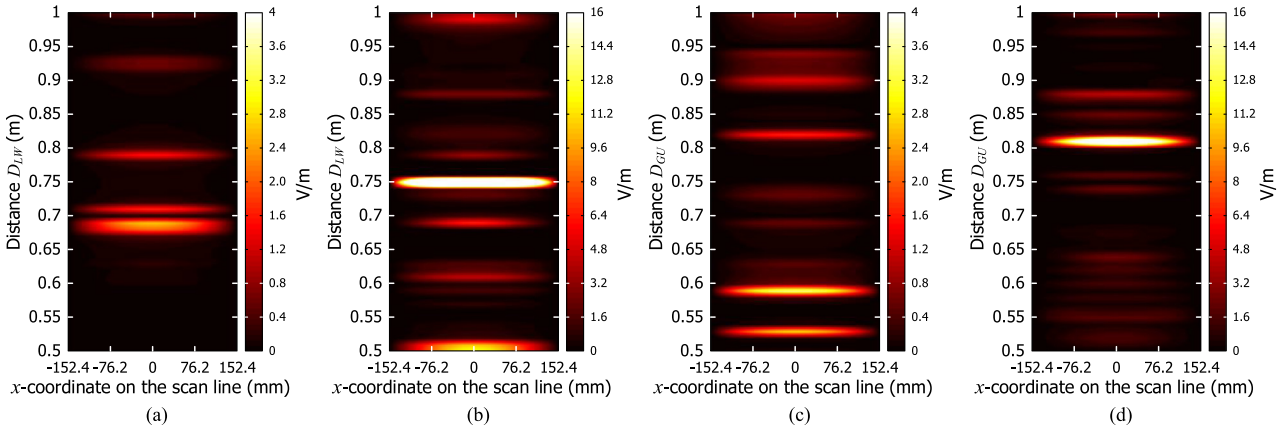

Fig. 3. Strengths and distributions of the electric field along the scan line while the distances from the lateral walls ($d_1 = d_2 = D_{LW}$) for $h_G = h_U = 1$ m increase from 0.5 to 1 m at (a) 500 MHz and (b) 1 GHz, and the distances from the ground and ceiling increases ($h_G = h_U = D_{GU}$) for $d_1 = d_2 = 1$ m at (c) 500 MHz and (d) 1 GHz ($w = 0.3048$ m (12 inch), $h_1 = h_2 = 0.1016$ m (4 inch), $c = 0.305$ m, and $t = 0.005$ m).

precautions against potential EMI should be prepared to protect electromagnetically the cable trays in the high-frequency regime (i.e., >1 GHz). To clarify the important points affected by the coupled electric fields, we summarized the information depending on the analysis conditions in Fig. 3. In Table 2, the distances D_{LW} and D_{GU} represents where the electric fields in the middle of the victim cable tray are more than 1 V/m at 500 MHz and 4 V/m at 1 GHz, respectively. Consequently, it is necessary to avoid the tabulated distances D_{LW} and D_{GU} in Table 2 when vertically installing the cable trays in parallel.

Next, the electric-field strength along the scan line when the surrounding architectural structures are asymmetric with respect to the cable trays (i.e. $d_1 \neq d_2$ and $h_G \neq h_U$) was investigated similarly. Fig. 4 shows the resulting electric-field strengths along the scan line at 500 MHz and 1 GHz, while either distance d_1 or h_G changes from 0.5 to 1.5 m. Fig. 4(a) and (b) show that the electric-field strength in the victim cable tray varies as a function of the distance d_1 at 500 MHz and 1 GHz, respectively, while the location on x-axis changes for a constant distance d_1. In Fig. 4(a) and (b), the structural asymmetry (i.e. $d_1 \neq d_2$) results in an asymmetric electric-field distribution. Therefore, the overall electric field in the victim cable tray should be investigated to avoid the EMI problem when cable trays are not installed in the middle from both lateral walls. Moreover Fig. 4(c) and (d) show that the electric field coupled in the victim cable tray at 500 MHz is less than E_{MA}, whereas that at 1 GHz exceeds E_{MA} for distances h_G of 0.6, 0.88, and 1.06 m. Thus, it is recommended that cable trays be installed with a distance h_G of more than 1.06 m to protect the cable trays from potential EMI problems.

4. Conclusion

A mode-matching method was applied for the estimation of the EM coupling between open cable trays within an indoor structure. The Helmholtz equation, in conjunction with the separation of variables, was used to derive the mathematical series expression

Table 2
Distances D_{LW} and D_{GU} where the electric field in the middle of the victim cable tray exceeding 1 V/m at 500 MHz and 4 V/m at 1 GHz.

Figure	Distance D_{LW} or D_{GU}	Electric-field strength
Fig. 3(a)	$D_{LW} \approx$ 0.69, 0.71, and 0.79 m	over 1 V/m (@ 500 MHz)
Fig. 3(b)	$D_{LW} \approx$ 0.5, 0.61, 0.69, 0.75, 0.79, and 0.99 m	over 4 V/m (@ 1 GHz)
Fig. 3(c)	$D_{GU} \approx$ 0.53, 0.59, 0.82, and 0.9 m	over 1 V/m (@ 500 MHz)
Fig. 3(d)	$D_{LW} \approx$ 0.81 and 0.88 m	over 4 V/m (@ 1 GHz)

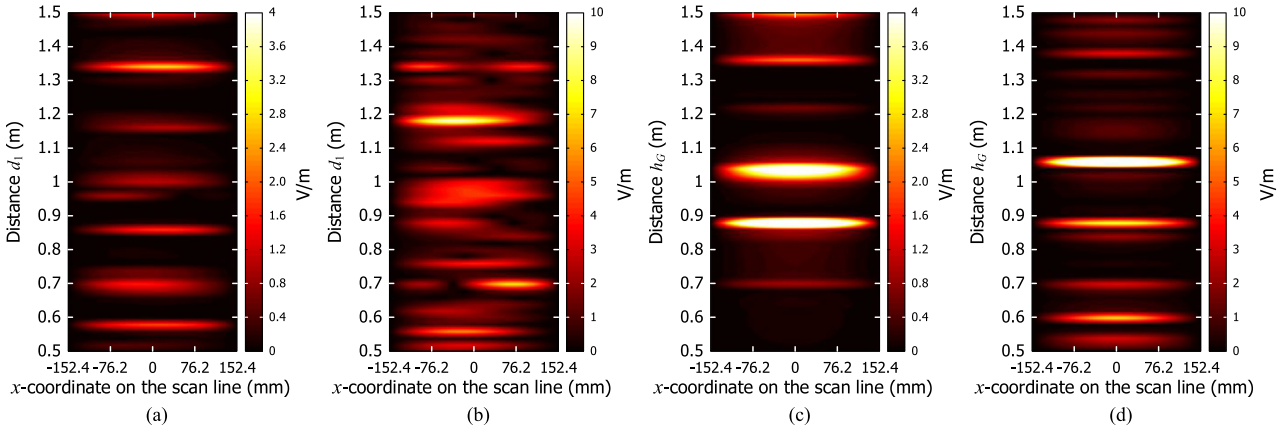

Fig. 4. Strengths and distributions of the electric field along the scan line while the distance d_1 from the lateral walls ($d_2 = h_G = h_U = 1$ m) increases from 0.5 to 1.5 m at (a) 500 MHz and (b) 1 GHz, and as the distance h_G from the ground increases ($h_U = d_1 = d_2 = 1$ m) at (c) 500 MHz and (d) 1 GHz ($w = 0.3048$ m (12 inch), $h_1 = h_2 = 0.1016$ m (4 inch), $c = 0.305$ m, and $t = 0.005$ m).

with the unknown modal coefficients to represent electromagnetic fields. Then, the modal coefficients were determined from the boundary conditions for electric- and magnetic-field continuities. Using the obtained modal coefficients, the distribution of the electric field strength in a victim cable tray was investigated as a function of the distances between cable trays and architectural surfaces. We found that the electric field strength in the victim cable tray changes to be strong as an interested frequency increases or the distances from architectural surfaces change. Before cable trays are installed, it is recommended that to investigate the EMI circumstance at the interested frequency band with the change of the distances from surrounding objects. The investigated results can provide useful information for preventing EMI problems between open cable trays.

Declaration of competing interest

The authors declare that they have no known competing financial interests or personal relationships that could have appeared to influence the work reported in this paper.

Acknowledgement

This work was supported by the Nuclear Safety Research Program through the Korea Foundation Of Nuclear Safety (KoFONS) using the financial resource granted by the Nuclear Safety and Security Commission (NSSC) of the Republic of Korea. (No. 2106005).

References

[1] M.J.A.M. van Helvoort, Grounding Structure for the EMC-Protection of Cabling and Wiring, Ph.D. Dissertation, Eindhoven Univ. Technol., 1995.
[2] N.W. Ebertsohn, R.H. Geschke, H.C. Reader, Cable trays in EMC: measurement and modeling to 30 MHz, IEEE Trans. Electromagn C. 49 (2007) 346–353.
[3] P.S. van der Merwe, H.C. Reader, D.J. Rossouw, Cable tray connections for electromagnetic interference (EMI) mitigation, IEEE Trans. Electromagn C. 53 (2011) 332–338.
[4] D. Zhang, Y. Wen, Y. Wang, D. Liu, X. He, J. Fan, Coupling analysis for wires in a cable tray using circuit extraction based on mixed-potential integral equation formulation, IEEE Trans. Electromagn C. 59 (2017) 862–872.
[5] U.S. NRC, Criteria for independence of electrical safety system, Regulatory Guide 1 (75) (2005).
[6] IEEE, IEEE standard criteria for independence of class 1E equipment and circuits, IEEE Standard 384 (2008).
[7] J. Choo, H.-K. Lee, J.-E. Park, H. Choo, Y.-H. Kim, Analysis of electromagnetic interference between open cable trays, IEEE Access 8 (2020) 72275–72286.
[8] H.J. Eom, Wave Scattering Theory, Springer Verlag, Berlin, 2001.
[9] *COMSOL Multiphysics* 5.4, https://www.comsol.com.
[10] U.S. NRC, Guideline for evaluating electromagnetic and radio-frequency interference in safety-related instrumentation and control systems, Regulatory Guide 1 (180) (2003).